

# Fabrication strategies and potential applications of the “green” microstructured optical fibers

Alexandre Dupuis  
Ning Guo  
Yan Gao  
Olga Skorobogata  
Bertrand Gauvreau  
Charles Dubois  
Maksim Skorobogatiy  
École Polytechnique de Montréal  
Engineering Physics Department  
Montréal, Québec H3T 1J4  
Canada

**Abstract.** Biodegradable microstructured polymer optical fibers have been created using synthetic biomaterials such as poly(L-lactic acid), poly( $\epsilon$ -caprolactone), and cellulose derivatives. Original processing techniques were utilized to fabricate a variety of biofriendly microstructured fibers that hold potential for *in vivo* light delivery, sensing, and controlled drug-release. © 2008 Society of Photo-Optical Instrumentation Engineers. [DOI: 10.1117/1.2978062]

Keywords: fiber optics; fiber application; biomedical optics; polymers; fiber characterization.

Paper 08015RR received Jan. 14, 2008; revised manuscript received Apr. 7, 2008; accepted for publication Apr. 10, 2008; published online Sep. 18, 2008.

## 1 Introduction

Biomaterials, or synthetic biodegradable polymers, have proven to be extremely useful for a wide range of health applications, such as medical products (surgical implants, sutures, fracture fixation devices), scaffolds for tissue engineering, and formulations for controlled drug-release therapies.<sup>1–7</sup> Independently, the field of microstructured polymer optical fibers (MPOFs) has grown tremendously in the past few years.<sup>8–11</sup> Polymer optical fibers offer many unique advantages, such as low cost, biofriendly material combinations, and the possibility of tailoring fiber-optical properties through doping, polymer functionalization, and fiber geometry manipulation. This versatility in the composition and processability of polymers has led to a wide variety of new geometries for microstructured optical fibers, allowing integration of several functionalities into the same fiber beyond simple optical guidance. We believe that the marriage of biomaterials and microstructured optical fibers (“green” fiber optics) opens a new venue for the application of optical fibers in medicine, notably for *in vivo* sensing and imaging, controlled drug delivery, and power delivery for laser surgery. In this paper, we present several original strategies for the preform fabrication and drawing of structured polymer optical fibers using, exclusively, biopolymers.

We start with a brief review of the MPOF potential applications in the biomedical field. Immediately after the discovery of the silica glass microstructured fibers, their unique advantages in optical sensing were recognized.<sup>12–14</sup> Consequently, polymer microstructured fibers were developed for biomedical sensing in view of the fiber biofriendly material combination. Among the first applications of MPOFs was fluorescence detection of antibodies.<sup>10,15,16</sup> In such fibers, a sample to be analyzed can be pumped through the hollow microstructure of a porous fiber and antibodies labeled with fluorescent markers can be selectively captured by an appropriately functionalized surface. Evanescent coupling of the fluorescent light into the fiber core can then be used for the

detection of binding events. Furthermore, functionalization of a polymer surface with biosensitive layers was found to be considerably easier than a glass one.<sup>10</sup> The *in vivo* sensing would also be facilitated if probing light could be confined directly to an aqueous analyte-filled core. High sensitivity of such analyte-filled structures has indeed been demonstrated with porous optical fibers.<sup>13,17–19</sup> Recently, microstructured dual-core optical fibers<sup>20,21</sup> have been used for enhancing the sensitivity of fluorescence microscopy, as such a structure permits high optical intensity single-mode delivery of the excitation pulse through a smaller core, and efficient multimode collection of the signal (fluorescent light) by the larger core of higher numerical aperture.<sup>20</sup> To further enhance sensitivity, it has recently been suggested to combine photonic crystal microstructured fibers with metal layers to enable resonant detection of plasmonic excitations.<sup>22</sup> Such metallized fibers were proposed to be used for the label-free, ultrasensitive detection of biomolecular binding events. For high-power laser delivery, hollow core microstructured fibers, which minimize bulk absorption losses by propagating principally in a gas-filled core, have been demonstrated to deliver tens of watts of laser power almost anywhere in the visible and IR. Particularly, plastic Bragg fibers<sup>23</sup> have been shown to enable flexible delivery of power from Nd:YAG, Er:YAG, and CO<sub>2</sub> lasers. Finally, fibers with a water-soluble microstructure hold a tremendous potential for monitored drug delivery.<sup>11</sup> Thus, impregnation of soluble microstructure with active pharmaceuticals, such as anesthetics or antibiotics, allows their slow release when the fiber is placed into the aqueous environment. The remaining concentration of the pharmaceuticals can be controlled by registering changes in the fiber-optical response due to dissolution of the fiber microstructure.

In this paper, we report fabrication of the fibers guiding by the total internal reflection mechanism. In such fibers, the light is confined to the higher refractive index core, which is surrounded by the lower refractive index cladding. Table 1 gives a list of biodegradable polymers studied in this paper and presents some of their physical and optical properties.

Address all correspondence to: M. Skorobogatiy, Engineering Physics Department, École Polytechnique de Montréal. E-mail: maksim.skorobogatiy@polymtl.ca.

**Table 1** Properties of the common biodegradable polymers.

Polymer	Abbr.	Refractive Index	$T_g$ (°C)	$T_m$ (°C)
Cellulose Acetate	CA	1.48	150	—
Cellulose Butyrate	CB	1.48	100	—
Hydroxypropyl Cellulose	HPC	1.34	120	—
Poly ( $\epsilon$ Caprolactone)	PCL	1.52	-60	60
Poly(L-Lactic Acid)	PLLA	1.45	57	152

## 2 Fiber Fabrication Strategies

Optical fibers are drawn from large-scale preforms, which are cylinders having the cross section of a desired fiber geometry. The preform is heated in the furnace of a drawing tower, and the fiber is drawn at a constant speed to reduce its diameter to the desired size. The reduction is essentially homothetic provided that the thermal expansion coefficients of the preform polymers are similar. The quality of the resulting fiber depends greatly on the quality of the prepared preform. This study explores three techniques to process biomaterials into fiber preforms: the corolling of polymer films, powder filling, and solution casting. In Fig. 1 we present schematics of the

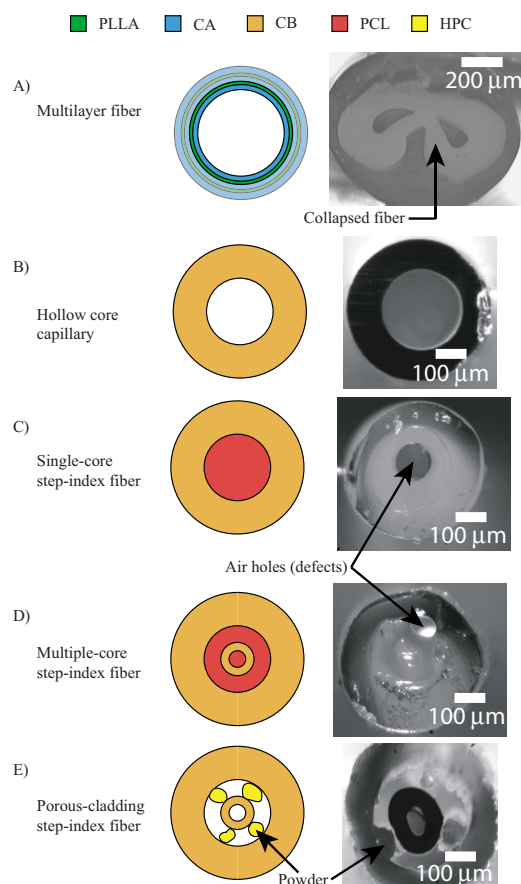


**Fig. 1** Schematics of the preform geometries and microscope images of the drawn fiber cross-sections using various fabrication strategies.

TIR fiber preforms, as well as the cross sections of drawn fibers.

### 2.1 Corolling Technique, Multilayer Fibers

We first describe a corolling technique<sup>24</sup> to fabricate multilayered all-polymer preforms containing several distinct materials in their cross section [Fig. 1(a)]. Thus, two or more polymer films having the desired thickness ratios are placed on top of each other and then jointly rolled around a mandrel. The rolled films are subsequently consolidated together by heating above the melting temperature in a vacuum oven. After cooling down, the mandrel is removed from the preform. Generally, the multilayer formed by the polymer films can be repeated after each turn around the mandrel, forming a periodic multilayer stack with any desired number of layers. During drawing, the central hole can be either collapsed or left open to result in the solid or hollow core multilayer fibers, known as Bragg fibers. Practical applications of Bragg fibers include light guidance in the hollow, solid, or liquid-filled cores for sensing and power delivery.<sup>23–25</sup>

The principal advantage of the corolling method is the simplicity with which a multimaterial periodic structure can be created, while the principal disadvantage of the method is the difficulty in managing contamination and nonuniformities due to the mechanical nature of the rolling process.<sup>25</sup> Moreover, in order to avoid delamination of the layers during drawing, it is desirable, although not critical, that the materials have similar melting temperatures. Another practical disadvantage of a corolling method is its reliance on the availability of high-quality polymer films. Thus, whereas most conventional polymers are commercially available in the form of films, for most biomaterials, such films are difficult to find.

A two-layer fiber preform was ultimately prepared by corolling the higher refractive index cellulose acetate (CA) film with the lower index poly(L-lactic acid) (PLLA) film around a 2-cm-diam Teflon rod. For preform fabrication, we used commercial 127- $\mu\text{m}$ -thick CA films purchased from McMaster-CARR. However we had to cast our own PLLA films. Several methods were tested to get thin films of PLLA. We first attempted to extrude the polymer but were only able to get thick films on the order of 1 mm. Therefore, we had to resort to solution casting of a 100- $\mu\text{m}$  film. The solution of PLLA was prepared by dissolving polymer pellets in a methylene chloride. PLLA pellets were purchased from Nature-Works. A solution was cast onto an 8  $\times$  13 in. glass sheet, with a Teflon's seal around the edge to prevent leakage. The thickness of the polymer film was controlled by the concentration of the solution. The film was dried at 40°C in a nitrogen atmosphere until it could be removed from the glass. The freestanding transparent PLLA film was subsequently dried in a vacuum oven at 120°C for three days.

We then proceeded with fabrication of a single bilayer fiber presented in Fig. 1(a). The rolled preform was mounted in the drawing tower and preheated at 150°C for 1 h. Thereafter, the temperature was ramped over 1 h to the drawing temperature of 225°C. Care should be taken not to overheat the preform because, at higher temperatures, PLLA tends to degrade with apparition of a brown color. The fiber was drawn at 225°C to a diameter of  $\sim 860 \mu\text{m}$ . During drawing, the bilayer structure has a tendency to collapse [see Fig. 1(a)]

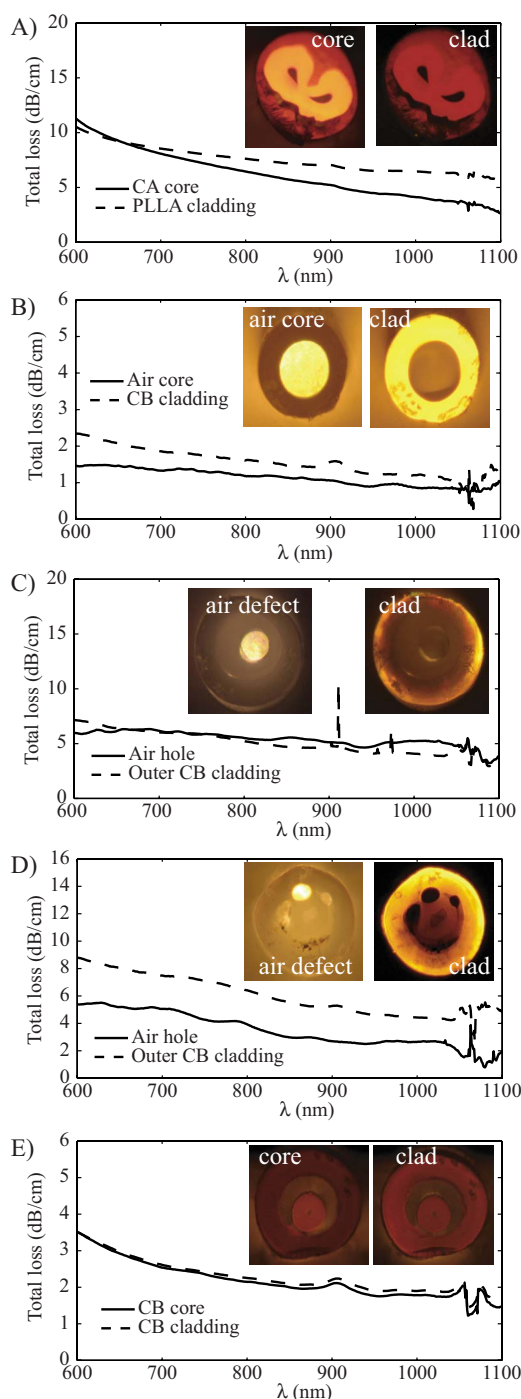


**Fig. 2** Transmission spectra of the biodegradable optical fibers with images of the transmitted light as insets. The fiber geometries are identified in Fig. 1. The lengths of the measured segments are 3.2, 6.95, 3.35, 3.25, and 8.05 cm respectively.

apparently due to the high surface tension of the polymers in a melted state.

Figure 2 reports measured transmission spectra of the studied fibers for the light launched either in the fiber core, cladding, or air hole. In the insets, the photos of the intensity distribution in the fiber cross sections are shown for different launch conditions. In all the optical characterization measurements, the fibers were cleaved with a hot razor blade cutting

at a constant speed and temperature. A supercontinuum white-light source was coupled into the fibers using a microscope objective. The output was sent into an Oriel Cornerstone monochromator, and the power at each wavelength was measured using a Si detector and a Newport powermeter. The resulting transmission spectra were normalized with respect to the spectrum of the supercontinuum in the absence of a fiber and the length of each fiber segment. The resulting total loss spectra, including the coupling loss, were plotted as a function of wavelength in Fig. 2. Ideally, the fiber losses would be measured by the standard cutback technique; however, the short length of the heavily multimode fibers makes this technique impractical.

In the inset of Fig. 2(a), we can see that the collapse of the bilayer structure has created a higher refractive index CA core region surrounded by the lower index PLLA cladding. Light guides much more efficiently in the CA than in the PLLA. From the normalized transmission data, and from the fiber length of 3.2 cm, we estimate the total loss in the CA region of the PLLA/CA fiber to be 9.8 dB/cm at wavelength 633 nm. These losses are attributable mostly to the structural inhomogeneities of the PLLA layer in the drawn fiber resulting from the low quality of a solution cast homemade PLLA film.

## 2.2 Powder Filling Technique, Single Core Fibers

We now discuss fabrication of the single-core step-index fibers [Fig. 1(c)] by filling a lower refractive index polymer tube [Fig. 1(b)] with a higher refractive index polymer powder. Cellulose butyrate (CB) was chosen as a tube material mainly because of its commercial availability. As a filling material for the interstitial region, higher refractive index poly( $\epsilon$ -caprolactone) (PCL) was chosen. Practical applications of a single-core step-index biodegradable fiber include disposable fibers for *in vivo* light delivery, or a controlled drug delivery, where fiber core is made of a water-soluble material doped with pharmaceuticals.

For the following experiments PCL powder was purchased from Sigma-Aldrich, while CB tubing was purchased from McMaster-CARR. We began by drawing single CB tubes [Fig. 1(b)] into capillaries to find the appropriate range of drawing parameters. Particularly, the CB capillaries of 393  $\mu\text{m}$  diam at a temperature of 178  $^{\circ}\text{C}$ , and a drawing speed of 1 m/min were fabricated. Interestingly, over the distances of several centimeters, such capillaries can guide light in their hollow cores as seen in Fig. 2(b) with an estimated loss of 1 dB/cm. CB appears to be the most transparent of the biodegradable polymers indicated in Table 1. Further measurement of the light guidance in a CB cladding of a 6.95-cm-long capillary lead to a 2.2-dB/cm fiber-loss estimate at wavelength 633 nm.

To fabricate a step index fiber preform [Fig. 1(c)], a CB tube having an inner and outer diameter of 3/8 and 5/8 in. was tightly packed with a higher refractive index PCL powder. The preform was solidified in a vacuum oven at 110  $^{\circ}\text{C}$ . It was then preheated in the draw tower at 130  $^{\circ}\text{C}$  for 3 h and drawn at 176  $^{\circ}\text{C}$  into 420- $\mu\text{m}$ -diam fiber.

Using this fabrication approach, it was difficult to prevent the formation of trapped air bubbles in the preform. An air-hole defect, which spans the entire length of the fiber segment, can clearly be seen in the resulting fiber [Fig. 1(c)].

Figure 2(c) shows the transmission spectrum of the step-index fiber. Whereas the air defect can guide some light, the PCL regions appear to be optically opaque and true guidance can only be observed by coupling into the CB regions. We estimate the loss in the outer CB cladding of this fiber of length 3.35 cm to be 6.7 dB/cm at wavelength 633 nm. We ascribe nontransparency of a PCL fiber core to the high degree of crystallinity in this material after preform consolidation, which can be also confirmed as a milky color of the resulting fibers. Better processing conditions of a PLC polymer to suppress its crystallization during preform fabrication are needed to perfect this approach.

### 2.3 Powder Filling Technique, Multiple Core Fibers

We now discuss fabrication of the multiple-core fibers (Figs. 1(d) and 1(e)). Such fibers can be fabricated by inserting a small-diameter tube within a larger diameter tube, and by filling the interstitial region between the tubes with an optically different material. The central hole of the inner tube can alternatively be filled, be left as an air hole, or be collapsed during the drawing process. As filling materials for the interstitial regions, higher refractive index PCL and lower refractive index hydroxypropyl cellulose (HPC) were used. Potential application of double-core fibers include enhanced *in vivo* sensing, where high intensity light is launched through a smaller core, while reflected light is collected efficiently through a larger core. Incorporation of the hollow or water-soluble microstructure into such fibers can also enable environment sampling and drug-delivery functionalities.

First multiple-core step-index fiber was created by inserting a small CB tube into a larger CB tube and by filling the interstitial region and the inner tube hole with higher refractive index PCL powder, thus forming two concentric PCL fiber cores. The smaller CB tube had inner and outer diameters of 1/8 and 1/4 in., whereas the larger tube had inner and outer diameters of 3/8 and 5/8 in., respectively. The PCL powder was tightly compacted, and care was taken to keep the inner tube centered. The preform was solidified in a vacuum oven at 80°C. The consolidated preform was then drawn at 178°C into a 410- $\mu\text{m}$ -diam fiber. Again, air-hole defects are clearly seen in the PCL regions of the resulting fiber [see Fig. 1(d)], and we were unable to observe any light transmitted through the highly crystalline PCL core [see Fig. 2(d)]. The loss in the outer CB cladding of this multiple-core fiber of length 3.25 cm was estimated to be 8.3 dB/cm at wavelength 633 nm.

For the second design of a two-core fiber, we filled the space between the CB tubes with a lower refractive index material, leaving the central CB tube empty. In this case, these are the CB tubes that form the two higher refractive index cores. For the lower index material, we chose HPC, which is a water-soluble derivative of cellulose commonly used in ophthalmology. HPC powder was purchased from Sigma-Aldrich. Interestingly, high-molecular-weight HPC has a higher glass transition temperature than CB, which opens the door to the innovative fiber designs. For example, by filling the space between the CB tubes with an HPC powder, and then by drawing the thus prepared preform at temperatures below the softening temperature of an HPC powder, one can create a fiber where the inner CB core is suspended inside of the outer

CB core by a porous water-soluble network of HPC particles as shown in Fig. 1(e).

The preform was made by filling the interstitial region between the two CB tubes with a polydispersed HPC powder of molecular weight 80,000. Note that the preform was not consolidated prior to drawing. The preform was preheated in the drawing tower furnace for 4 h starting at 140°C with a 10°C/h increase until drawing temperature of 180°C was reached. Fibers of 415- $\mu\text{m}$ -diam were drawn at 180°C. The fiber  $\sim 1\text{--}4$  dB/cm transmission loss is mostly attributable to the HPC particles forming a highly porous network of scatterers lining the inner fiber core. Transmission through such fibers suspended in the aqueous environment was detailed in Ref. 11, where the fiber potential for monitored drug release applications was demonstrated.

### 2.4 Solution Casting Technique

Alternatively, to realize the multiple-core fiber preforms discussed in the previous section, HPC can be dissolved in water, then filled between the CB tubes, and finally, reconstituted in a solid form by water evaporation in the vacuum oven. This is a solution casting method. Figure 2(e) shows thus fabricated fibers and the corresponding transmission spectra. We note that losses through the inner and outer cores are similar, with an estimated loss of 3.1 dB/cm at wavelength 633 nm as measured using an 8.05-cm-long fiber.

## 3 Discussion

To the best of our knowledge, this is the first time that polymer optical fibers have been attempted from a variety of biodegradable polymers. Although the total transmission losses of the examples presented above are high ( $\sim 1\text{--}10$  dB/cm), it is important to note that this is not the lower limit to the fiber transmission loss. This is because the intrinsic losses of biopolymers presented in this work are comparable in the visible and near-IR to other transparent plastics, such as PMMA, for example. The main reason why the losses of fibers in this work are so high is because the optical quality tubing, rods, and films made of biodegradable polymers are currently not commercially available. Therefore, we were forced to build our microstructured preforms starting from powders and granules using the best processing techniques we could envision. In contrast, most of the state-of-the-art low-loss polymer-microstructured fibers are currently built by stacking or otherwise manipulating optical quality commercial tubes and rods. If the same are available for biopolymers, low-loss microstructured biodegradable fibers will be much easier to manufacture.

Moreover, even using the preform fabrication strategies presented in this work, the current fiber losses can be reduced by mitigating various structural and material defects, as detailed in the text of the paper. For instance, while employing solution-casting and powder-filling techniques, we witnessed structural inhomogeneities in the solution-cast PLLA films, as well as high degree of crystallinity and trapped air bubbles within the powder-filled PCL region of a preform. Nevertheless, we believe that fibers of greater length and lower loss can be achieved by addressing these controllable processing difficulties.

Furthermore, in our opinion, one has to always leverage the advantages of different fibers. Even if the loss of a biodegradable fiber could be small, a realistic scenario for the use of such a fiber would probably be in combination with standard power delivery fibers, just because there are good commercial solutions for the power delivery, that are readily available. For biodegradable fibers, it is the potential *in vivo* aspect, which, in our opinion, is most promising. For example, if biofriendly fibers can be introduced directly into the human body, they could prove to be a more flexible and smaller light delivery solution than, for example, silica fibers, which although bionutral, are typically delivered within a larger endoscope superstructure.

Finally, we conclude with a rather intriguing observation that biodegradable polymers, which are typically perceived as rather fragile to work with, are actually robust enough so that they can be processed using well-developed and industrially sound fiber drawing techniques.

## 4 Conclusion

In summary, we have presented fabrication strategies of biodegradable and biocompatible microstructured plastic optical fibers using corolling of plastic films, powder-filling, and solution-casting techniques. Furthermore, we have demonstrated that industrially rugged process of fiber drawing from solid preforms can be applied to the mass production of such fibers. Potential applications of biofriendly fibers in *in vivo* sensing, imaging, controlled drug delivery, and high-power delivery were discussed. Particularly, microstructured fibers with functionalized hollow microstructure can be used *in vivo* for real-time detection of biomolecule binding events. Hollow core multilayer fibers can be used *in vivo* for high-power delivery of medically important lasers. Multicore step-index fibers can be used *in vivo* for fluorescence microscopy by delivering high power in a smaller core and collecting fluorescence in a larger core with higher NA. Microstructured fibers with impregnated water-soluble pharmaceuticals can be used *in vivo* for controlled drug delivery; monitoring of drug dispensation is achieved by detecting changes in the fiber-optical transmission properties. Finally, the *in vivo* direct use of biopolymer optical fibers promises a more compact alternative to the endoscopes.

## Acknowledgments

This work was supported by the Canada Research Chair Foundation and the FP3 project of Canada Institute for Photonics Innovations. We also thank Prof. Mark P. Andrews of McGill University for his insightful comments.

## References

1. M. Vert, S. M. Li, G. Spenlehauer, and P. Guerin, "Bioresorbability and biocompatibility of aliphatic polyesters," *J. Mater. Sci.: Mater. Med.* **3**, 432–446 (1992).
2. H. L. Wald, G. Sarakinos, M. D. Lyman, A. G. Mikos, J. P. Vacanti, and R. Langer, "Cell seeding in porous transplantation devices," *Biomaterials* **14**, 270–278 (1993).
3. G. J. Beumer, C. A. van Blitterswijk, and M. Ponec, "Degradative behaviour of polymeric matrices in (sub)dermal and muscle tissue of the rat: A quantitative study," *Biomaterials* **15**, 551–559 (1994).
4. J. A. Setterstrom, T. R. Tice, and W. E. Meyers, in *Recent Advances in Drug Delivery Systems*, S. W. Kim, Ed., p. 185, Plenum Press, New York (1984).
5. D. S. Katti and C. T. Laurencin, in *Advanced Polymeric Materials: Structure Property Relationship*, p. 479, CRC Press, Boca Raton (2003).
6. J. Heller, "Polymers for controlled parenteral delivery of peptides and proteins," *Adv. Drug Delivery Rev.* **10**, 163–204 (1993).
7. R. Langer, "New methods of drug delivery," *Science* **249**, 1527–1533 (1990).
8. M. A. van Eijkelenborg, A. Argyros, G. Barton, I. M. Bassett, M. Fellow, G. Henry, N. A. Issa, M. C. J. Large, S. Manos, W. Padden, L. Poladian, and J. Zagari, "Recent progress in microstructured polymer optical fibre fabrication and characterisation," *Opt. Fiber Technol.* **9**, 199–209 (2003).
9. A. Argyros, M. A. van Eijkelenborg, M. C. J. Large, and I. M. Bassett, "Hollow-core microstructured polymer optical fiber," *Opt. Lett.* **31**, 172–174 (2006).
10. J. B. Jensen, P. E. Hoiby, G. Emilianov, O. Bang, L. H. Pederson, and A. Bjarklev, "Selective detection of antibodies in microstructured polymer optical fibers," *Opt. Express* **13**, 5883–5889 (2005).
11. A. Dupuis, N. Guo, Y. Gao, S. Lacroix, C. Dubois, and M. Skorobogatiy, "The prospective for the biodegradable microstructured optical fibers," *Opt. Lett.* **32**, 109–111 (2007).
12. T. M. Monro, W. Belardi, K. Furusawa, J. C. Baggett, N. G. R. Broderick, and D. J. Richardson, "Sensing with microstructured optical fibres," *Meas. Sci. Technol.* **12**, 854–858 (2001).
13. J. M. Fini, "Microstructure fibres for optical sensing in gases and liquids," *Meas. Sci. Technol.* **15**, 1120–1128 (2004).
14. S. O. Konorov, A. M. Zheltikov, and M. Scalora, "Photonic-crystal fiber as a multifunctional optical sensor and sample collector," *Opt. Express* **13**, 3454–3459 (2005).
15. A. Duval, M. Lhoutellier, J. B. Jensen, P. E. Hoiby, V. Missier, L. H. Pedersen, T. P. Hansen, A. Bjarklev, and O. Bang, "Photonic crystal fiber based antibody detection," *Proc. IEEE Sens.*, 4122–1225 (2004).
16. L. Rindorf, P. E. Hoiby, J. B. Jensen, L. H. Pedersen, O. Bang, and O. Geschke, "Towards biochips using microstructured optical fiber sensors," *Anal. Bioanal. Chem.* **385**, 1370–1375 (2006).
17. F. M. Cox, A. Argyros, and M. C. J. Large, "Liquid-filled hollow core microstructured polymer optical fiber," *Opt. Express* **14**, 4135–4140 (2006).
18. C. Martelli, J. Canning, K. Lyytikainen, and N. Grothoff, "Water-core Fresnel fiber," *Opt. Express* **13**, 3890–3895 (2005).
19. G. Vienne, M. Yan, Y. Luo, T. K. Liang, H. P. Ho, and C. Lin, CLEO/PR, CWM1-1 (2005).
20. M. T. Myaing, J. Y. Ye, T. B. Norris, T. Thomas, J. R. Baker, Jr., W. J. Wadsworth, G. Bouwmans, J. C. Knight, and P. St. J. Russell, "Enhanced two-photon biosensing with double-clad photonic crystal fibers," *Opt. Lett.* **28**, 1224–1226 (2003).
21. L. Fu and M. Gu, "Double-clad photonic crystal fiber coupler for compact nonlinear optical microscopy imaging," *Opt. Lett.* **31**, 1471–1473 (2006).
22. B. Gauvreau, A. Hassani, M. F. Fehri, A. Kabashin, and M. A. Skorobogatiy, "Photonic bandgap fiber-based surface plasmon resonance sensors," *Opt. Express* **15**, 11413–11426 (2007).
23. G. Dellemann, T. D. Engeness, M. Skorobogatiy, and U. Kolodny, "Perfect mirrors extend hollow-core fiber applications," *Photonics Spectra* **37**, 60–64 (2003).
24. Y. Gao, N. Guo, B. Gauvreau, M. Rajabian, O. Skorobogata, E. Pone, O. Zabeida, L. Martinu, C. Dubois, and M. Skorobogatiy "Consecutive solvent evaporation and co-rolling techniques for polymer multilayer hollow fiber preform fabrication," *J. Mater. Res.* **21**, 2246–2254 (2006).
25. A. Dupuis, N. Guo, B. Gauvreau, A. Hassani, E. Pone, F. Boismenu, and M. Skorobogatiy, "Guiding in the visible with "colorful" solid-core Bragg fibers," *Opt. Lett.* **32**, 2882–2884 (2007).